

SINTERING EFFECT ON THE MICROSTRUCTURE AND MECHANICAL  
PROPERTIES OF ALLOY 718 PROCESSED BY POWDER INJECTION MOLDING

J. J. Valencia\*, J. Spirko\*, and R. Schmees\*\*

\*Concurrent Technologies Corporation, 1450 Scalp Avenue, Johnstown, PA 15904

\*\*United Technologies, Pratt & Whitney, West Palm Beach, FL 33410

Abstract

Powder injection molding (PIM) is an emerging technology for manufacturing gas turbine engine components. To evaluate superalloy alloy 718 for these applications, mechanical testing specimens were produced by PIM and sintered at various heating rates in a partial pressure of argon. Alloy 718 is difficult to process because a low melting point eutectic-Laves phase develops during the sintering process. The Laves phase prevents full densification and decreases the tensile properties. Heating ramp rates up to 15°C/min and a holding time of 6 hours prevented the formation of Laves phase during sintering. In the as-sintered condition, 99% of the theoretical density was achieved. After HIP and heat treatment, the tensile properties at room temperature and 650°C exceeded the minimum property requirements, while stress rupture time, high cycle fatigue, and creep properties met typical aerospace properties. Stress rupture elongation life was met with an additional delta heat treatment.

---

This work was conducted by the National Center for Excellence in Metalworking Technology, operated by Concurrent Technologies Corporation under contract No. N00140-92-C-BC49 to the U.S. Navy as part of the U.S. Navy Manufacturing and Technology Program

## Introduction

Wrought components made from alloy 718 have gained considerable acceptance in the manufacturing of high-performance turbine engine components. Many of these components are highly complex shapes which are very expensive to produce due to extensive machining. Casting does not yield material suitable for these applications because of segregation and microstructural inhomogeneity. The same is true of press and sinter P/M processes because of the shape complexity and dimensional tolerances which cannot be achieved without extensive machining operations.

Powder injection molding (PIM) is an emerging technology for the cost-effective production of large numbers of small metal parts. PIM also has the ability to manufacture components with complex geometry and very close dimensional tolerances. In spite of the obvious cost advantage, PIM has not been implemented for the production of alloy 718 turbine engine components. The reasons for this are because of the stringent mechanical property requirements for aerospace components, and the very limited engineering knowledge database of PIM alloy 718 [1-3].

The objective of this work is to optimize the thermal consolidation of PIM alloy 718 to achieve the mechanical property requirements of aerospace material specification AMS 5596 [4]. To do this, the effect of sintering parameters on the microstructure and mechanical properties are examined.

## Experimental Procedures

A PIM feedstock was prepared from gas-atomized alloy 718 powder with a mean particle size of 15  $\mu\text{m}$  and a proprietary polymer-based binder to approximately 64% solids loading [5]. Tensile, stress rupture, creep, and high-cycle fatigue specimens were injection-molded to dimensionally comply with the ASTM standards. The specimens were solvent debound followed by thermal debinding and pre-sintering at 1090°C for 2 hours in a hydrogen atmosphere.

Sintering was conducted at 1260°C for 6 hours in vacuum with an argon partial pressure of approximately 1000 microns of mercury to prevent chromium evaporation of the alloy. To achieve the maximum sintering temperature, three heating ramp rates from room temperature were used including (1) 1°C/min, (2) 10°C/min, and (3) 15°C/min. The sintered specimens were hot isostatically pressed (HIP) at 1190°C for 4 hours at 103.5 MPa (15 Ksi).

Heat treatment was conducted per AMS 5663 specification [4]. Solution treatment was performed at 950°C for 1 hour in argon followed by air cooling. Precipitation treatment was conducted at 718°C for 8 hours, followed by furnace cooling at 38°C per hour to 620°C, holding for 8 hours, and then air cooling. Prior to the solution heat treatment, the stress rupture specimens were heat-treated at 870°C for 10 hours to increase the amount of the orthorhombic  $\text{Do}_a$  structure, or equilibrium  $\text{Ni}_3\text{Nb}$   $\delta$ -phase at the grain boundaries.

The specimen density was measured by the Archimedes method. Tensile properties were measured at room temperature and at 650°C. Stress rupture, high-cycle fatigue (HCF), and creep were also measured at 650°C. Microstructural analyses were conducted on selected samples using optical metallography and scanning electron microscopy (SEM) coupled with energy dispersion spectroscopy (EDS). Fracture analysis was performed by SEM.

## Results and Discussion

### Sintering Effects on Density and Microstructure

Table I compares the effect of the sintering rate on the density of the PIM alloy 718 sintered at 1260°C for 6 hours. The table also shows the heat treatment (HT) effect on the density for the various materials. The HIP effect on density is only shown for the alloy heated at a ramp rate of 15°C/min. The density of the heat-treated wrought alloy 718 is also provided for comparison.

The lowest as-sintered density was observed at a heating rate of 10°C/min, and the highest was obtained at 15°C/min. HT+HIP increased the sintered density at all ramp rates. However, the density of wrought alloy 718 is still higher than any of the PIM specimens.

Table I - Effect of Sintering Heating Rate on Density of PIM Alloy 718 Sintered at 1260°C for 6 Hours.

Sintering Heating Ramp Rate (°C/min)	Material Condition	Density (g/cm <sup>3</sup> )
1	As-Sintered	8.17
	HT	8.20
	HIP	8.27
10	As-Sintered	8.11
	HT	8.18
	HIP	8.21
15	As-Sintered	8.20
	HT	8.21
	HIP	8.26
Wrought AMS 5663	HT	8.3

Early studies showed that density increases with an increase in the heating ramp rate during the sintering process [2]. In the present work, this observation is confirmed from 10°C/min to 15°C/min. However, the heating ramp rate of 10°C/min yielded the lowest sinter density. One explanation for this observation is the formation of heavy intermetallic Nb-bearing  $\gamma$ /Laves eutectic phase at ~1170°C [2, 6-8] which remains liquid at the sintering temperature. Also, the high content of heavy elements such as niobium and chromium in the Laves phase slows its dissolution into the matrix. At 1°C/min ramp rate, the Laves phase was formed; however, there was sufficient time to dissolve a relatively large amount of this phase into the matrix. While at 15°C/min, the Laves phase does not have sufficient time to nucleate and grow in a significant proportion. Therefore, it is reasonable to assume that undissolved liquid eutectic Laves phase (particularly at a heating rate of 10°C/min) causes porosity during cooling. Figure 1 shows the microstructures for the various sintering rates.

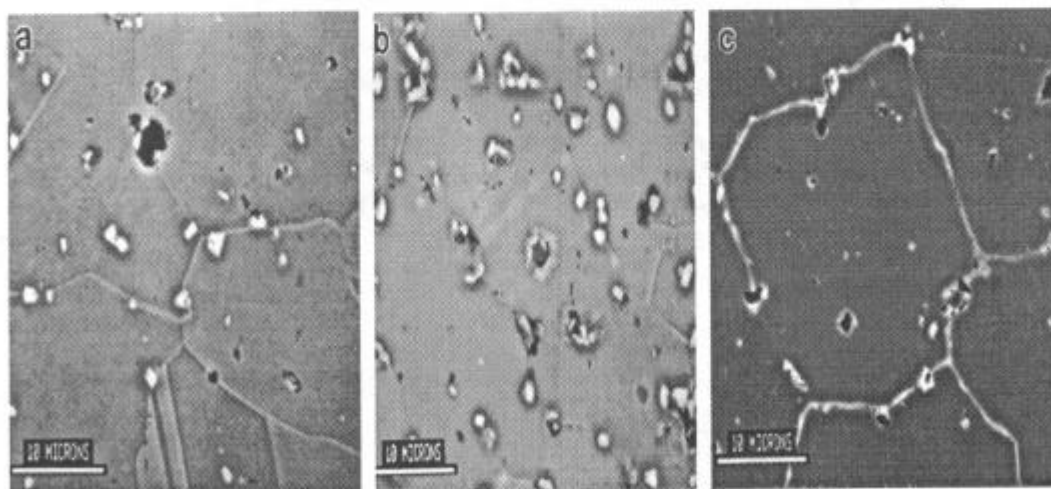


Figure 1 - SEM views of PIM alloy 718 in the as-sintered condition: (a) 1°C/min. (b) 10°C/min. (c) 15°C/min.

Note that the porosity is associated with the eutectic Laves phase primarily at 10°C/min. (Figure 1b). The eutectic Laves at 10°C/min. and 15°C/min. heating rates were found in a very small proportion (< 0.5 percent).

Table II shows the effect of the heating rate on the PIM 718 microstructure including total fraction of second phases (primarily identified as Laves and  $\delta$  phases), average grain size, and grain-size range. Note that the proportion of Laves and  $\delta$  phases was higher at 10°C/min and lower at 15°C/min. HIP+HT increased the amount of the second phases; however, at 1°C/min there is practically no change. A non-uniform grain size was observed in all as-sintered materials. However, the average grain size decreased with an increase in the sintering rate. HIP+HT had a minor effect on the grain size. These microstructural characteristics are shown in Figure 2.

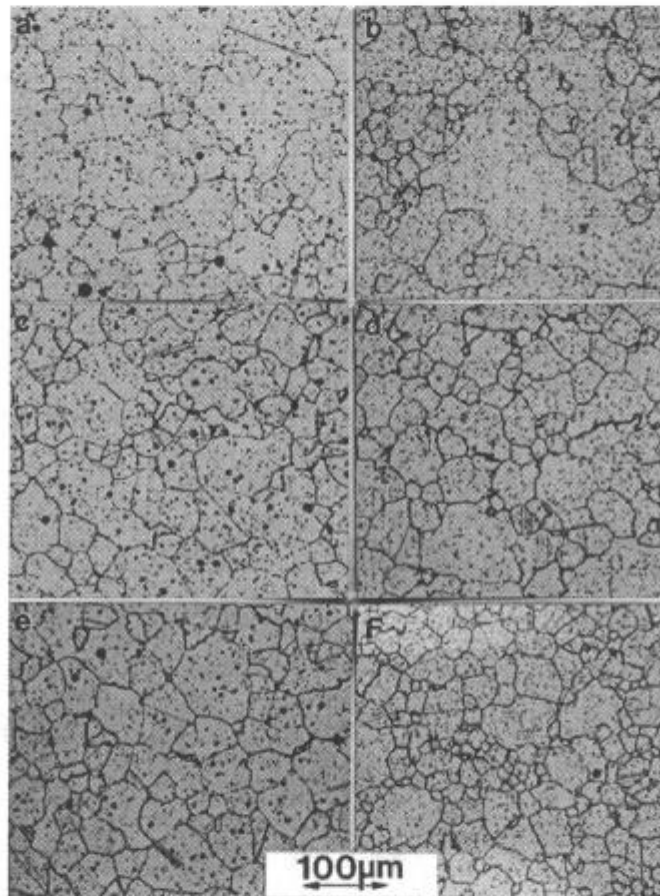


Figure 2 - Light optical views of PIM alloy 718 in the HT and HIP+HT conditions: (a) and (b) 1°C/min.; (c) and (d) 10°C/min.; (e) and (f) 15°C/min. (HT: left, HIP and HT: right)

Table II - Microstructural Characteristics of PIM Alloy 718

Sintering Rate (°C/min)	Condition	Laves and $\delta$ phases (%)	Average Grain Size ( $\mu\text{m}$ )	Grain Size Range ( $\mu\text{m}$ )
1	As-Sintered	$0.96 \pm 0.20$	43.4	10 - 300
	HIP +HT	$0.82 \pm 0.21$	40.6	10 - 250
10	As-Sintered	$1.20 \pm 0.40$	37.0	5 - 60
	HIP +HT	$1.50 \pm 0.23$	42.0	10 - 70
15	As-Sintered	$0.42 \pm 0.09$	28.0	5 - 80
	HIP +HT	$1.25 \pm 0.24$	25.6	10 - 100

The HIP+HT produced a more uniform distribution of the second phases at all sintering rates. EDS analyses shows that a large proportion of the second phases in the HIP+HT materials is the  $\delta$  phase. This is expected since some of the Laves phase was dissolved during holding at the HIP temperature (1190°C for 4 hours). Then the  $\delta$  phase was formed during the slow cooling of the HIP furnace from above the  $\delta$  solvus (~1020°C) [9]. The  $\delta$  phase had two morphologies which included a plate-like morphology that was found at the grain boundaries, and a globular morphology which was found intragranularly. The Laves phase persisted after HIP and heat treatment. However, the larger proportion of this phase was found in specimens sintered at a heating ramp rate of 10°C/min.

From all the PIM materials, the specimens sintered at a heating ramp rate of 10°C/min showed a more uniform grain size (Figures 2c and 2d). This may be due to the larger proportion of Laves and  $\delta$  phases (primarily Laves in this case) produced during the sintering process. As shown in Figure 3, a small grain size is associated with the presence of Laves phases, which are present at the grain boundaries; this suggests that Laves phases control the grain growth during sintering.

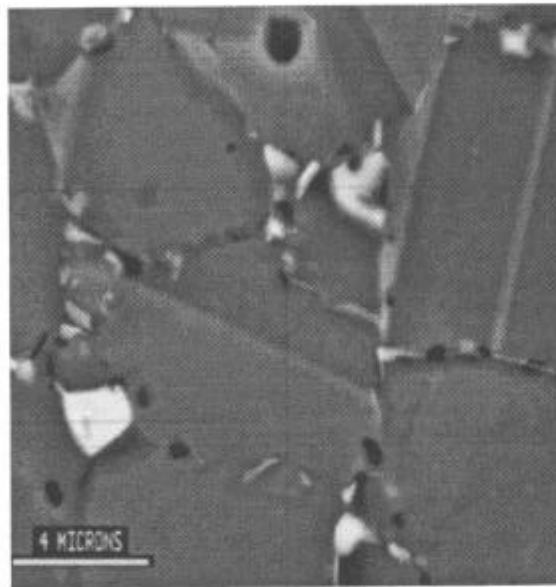


Figure 3 - SEM view of a PIM alloy 718 sintered at a heating rate of 15°C/min showing Laves phase at the grain boundaries.

### Mechanical Properties

#### Tensile Properties.

The effects of surface grinding on the testing specimens, as well as the effect of testing temperature on the mechanical properties, have been discussed in a previous paper [3]. The mechanical testing results presented here are discussed in terms of microstructure and sintering processing. In this study, it was observed that the specimens developed a surface texture during sintering. This is shown in Figure 4. The room temperature tensile testing results for the various heating rates were obtained from as-processed specimens. The surface texture was removed from the specimens by grinding before measuring the mechanical properties at high temperature.

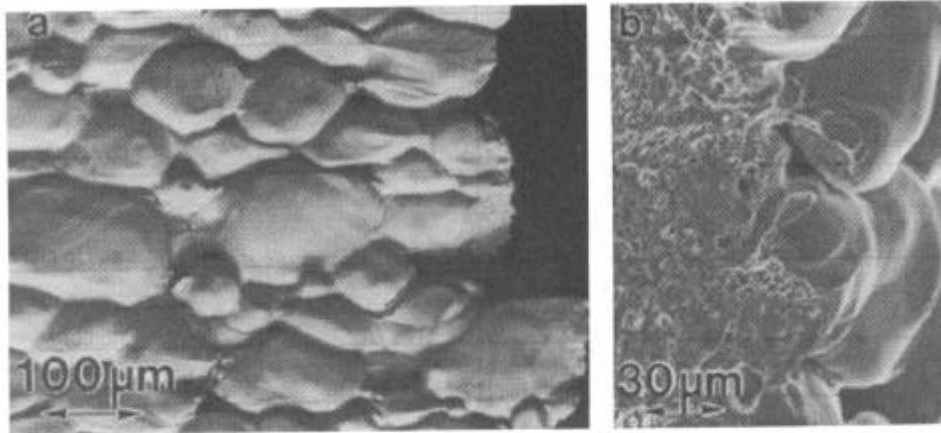


Figure 4 - SEM view showing the surface texture of a tensile specimen of PIM alloy 718:  
(a) general view (b) fracture surface.

Table III - shows the yield strength (YS), ultimate tensile strength (UTS), and percent elongation for the heat-treated and HIP+HT materials processed at the various heating rates. The minimum AMS 5662G requirements are also shown in Table III for comparison.

Table III Room Temperature Tensile Properties of PIM alloy 718 after precipitation heat treatment and HIP+HT.

Heating Ramp Rate (°C/min)	Condition	YS	UTS	Elongation (%)
1.0	HT	1088.0	1297.6	13.3
	HIP+HT	1086.6	1299.0	14.1
10.0	HT	1063.2	1206.6	9.4
	HIP+HT	1096.3	1292.8	11.6
15.0	HT	1061.8	1237.6	11.4
	HIP+HT	1133.1	1350.0	14.2
AMS 5662G [4] Minimum Requirements	HT	1034.2	1241.1	12.0

All materials exceeded the YS and UTS AMS 5662 minimum requirements. The highest ductility in the HT condition was found at a sintering heating rate of 1°C/min. However, the best combination of properties are obtained from the HIP+HT materials sintered at a heating rate of 15°C/min. The sintering heating rate of 10°C/min produced the lowest ductility in both HT and HIP+HT conditions. This is presumably due to the lower density caused by the large proportion of Laves phases formed at this heating rate. This also suggests that the Laves phases were not completely dissolved in the  $\gamma$ -matrix during solution treatment at high temperature or during HIPing.

Density, microstructure, and room temperature tensile strength provided the basis for selecting the sintering conditions for PIM alloy 718. Based on the results, the best combination of microstructure and properties was obtained at a heating rate of 15°C/min. This heating rate was used to consolidate the high temperature tensile, stress rupture, creep, and high-cycle fatigue specimens.

#### Tensile Properties at 650°C.

Table IV compares the average tensile properties at 650°C of PIM alloy 718 (as-processed and surface ground specimens) with the AMS 5596 minimum requirements. In each case, the YS, UTS, and elongation were above the AMS minimum requirements. Note that surface grinding had a minor effect on the tensile properties. Similarly, the surface texture had practically no effect on the room temperature tensile properties [3].

Table IV - Average Tensile Properties of PIM Alloy 718 and AMS 5596 Minimum Requirements at 650°C

Material	YS	UTS	Elongation (%)
PIM As-Processed	904.6 ± 17.0	1050.0 ± 8.2	9.7 ± 0.42
PIM Ground	910.0 ± 7.3	1047.4 ± 7.0	9.8 ± 0.05
AMS 5596	827.4	999.8	5.0

### Stress Rupture

Table V shows the results from the stress rupture testing conducted at 650°C and 689.5 MPa for the PIM HT and PIM HIP+HT, and heat-treated to precipitate  $\delta$ -phase ( $\delta$ -HT). The results are compared with the AMS 5596 minimum requirements. The PIM specimens were ground to remove the surface texture (Figure 4) in order to avoid premature failure of the specimens.

The results in Table V indicate that the PIM material in the HIP+HT condition did not meet the ductility requirements. However, the time it took to rupture exceeds the ductility requirements by a factor of at least 2.3 hours. The  $\delta$  heat-treated material showed the best results. The ductility meets or exceeds the minimum requirements, while the time it took to rupture increased by at least 50%.

Table V - Average Stress Rupture of Surface Ground PIM HIP+HT, HIP+ $\delta$ -HT, and AMS 5596 Tested at 650°C and 689.5 MPa

Material	Final Elongation (%)	Time to Rupture (hours)
PIM HIP + HT	2.85 ± 0.67	56.9 ± 6.13
PIM HIP + $\delta$ -HT	5.4 ± 1.0	35.9 ± 0.62
AMS 5596 minimum	4.0	23.0

Figure 5 shows the effect of the  $\delta$ -phase content on the stress rupture ductility for the PIM materials. Note that the ductility increases as the  $\delta$ -phase increases. The highest ductility (6.6%) was found in the PIM HIP+ $\delta$ -HT material which contained 15.2% of  $\delta$ -phase. The results obtained here are in good agreement with other observations on the stress rupture ductility [10, 11].

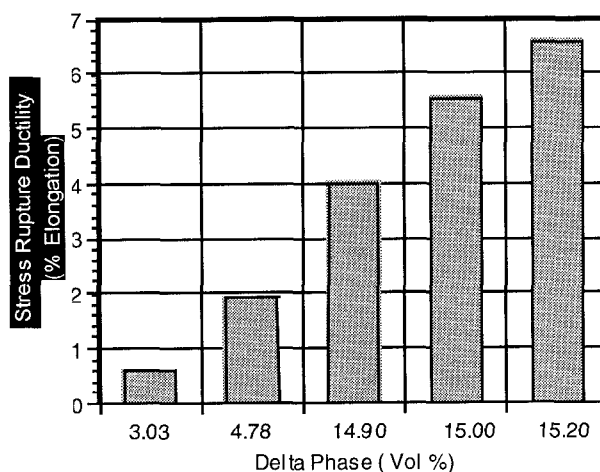


Figure 5 - Effect of the  $\delta$ -phase content on the stress rupture ductility of PIM alloy 718.

The  $\delta$ -phase has a positive influence on the stress rupture of alloy 718. However, it is expected that this phase has a detrimental effect on the yield strength. For instance, a decrease of 10% in



YS in forged alloy 718 containing mostly  $\delta$ -phase has been observed [14]. This decrease is attributed to the lack of sufficient  $\gamma'$  ( $\text{Ni}_3\text{Nb DO}_{22}$  structure). If this is the case based on the room temperature results, the PIM materials exceed the AMS minimum requirements by approximately 10%. Therefore, it is reasonable to assume that the YS of the PIM HIP+ $\delta$ -HT material will just meet the AMS minimum requirements.

Typical microstructures of the PIMed materials which were heat treated by the conventional process [4], and in the  $\delta$ -phase field are shown in Figure 6. In both materials, the major proportion of plate like  $\delta$ -phase is found at the grain boundaries. Also, a small proportion of  $\delta$ -phase is found intragranularly. Interestingly, both materials have the intragranular  $\delta$ -phase with two distinct plate and globular-like morphologies (Figures 6b and 6d). The globular like  $\delta$ -phase may be due to the presence of Laves phases; however, its origin is still uncertain.

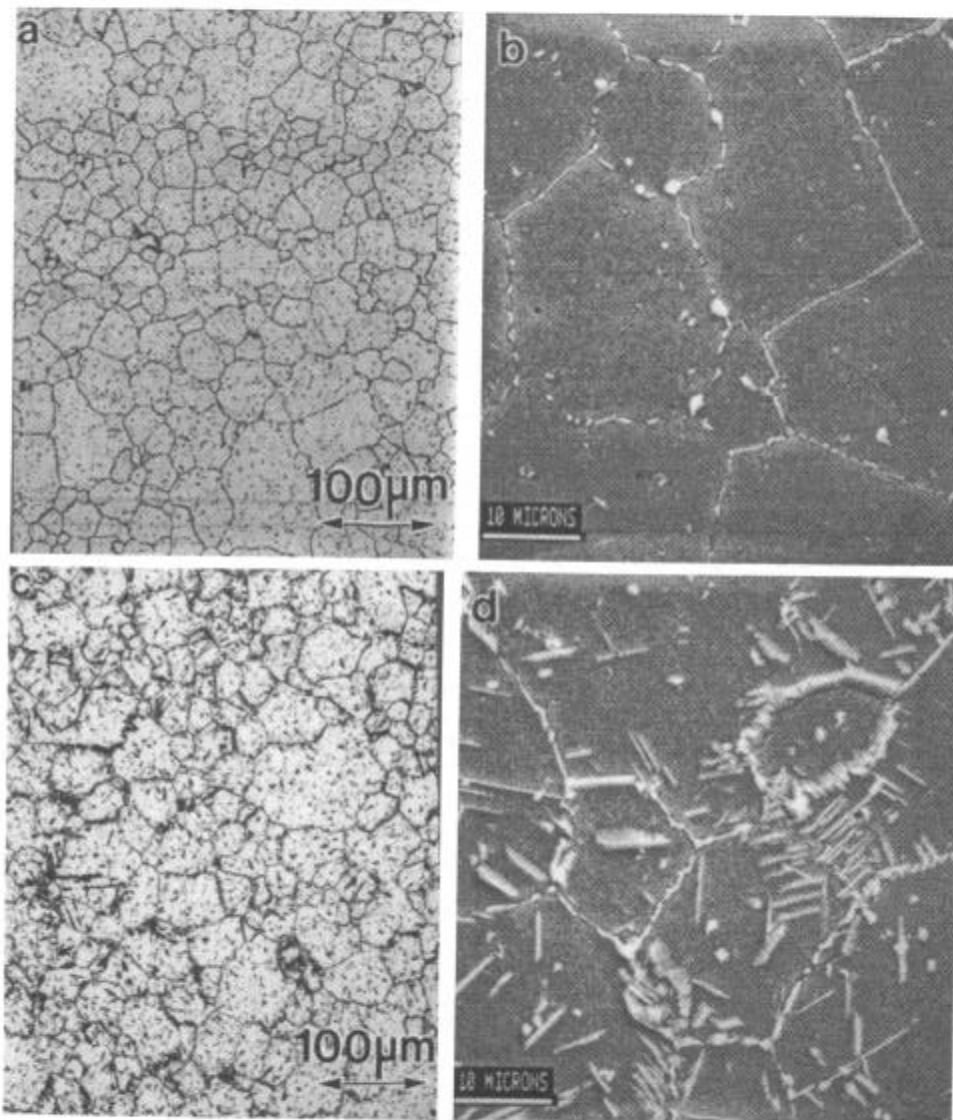


Figure 6 - Optical and SEM views of the microstructures of the PIM alloy 718: (a) and (b) conventionally HT (c) and (d)  $\delta$ -phase heat treated.

Another interesting feature of the PIM materials is that some of the grain boundary  $\delta$ -phase appears to be nucleated at Laves phases as shown in Figure 7. This may be due to the high



niobium concentration of the Laves phases. Nevertheless, the presence of globular-like and grain boundary  $\delta$ -phase which is associated with Laves phases deserves further investigation.

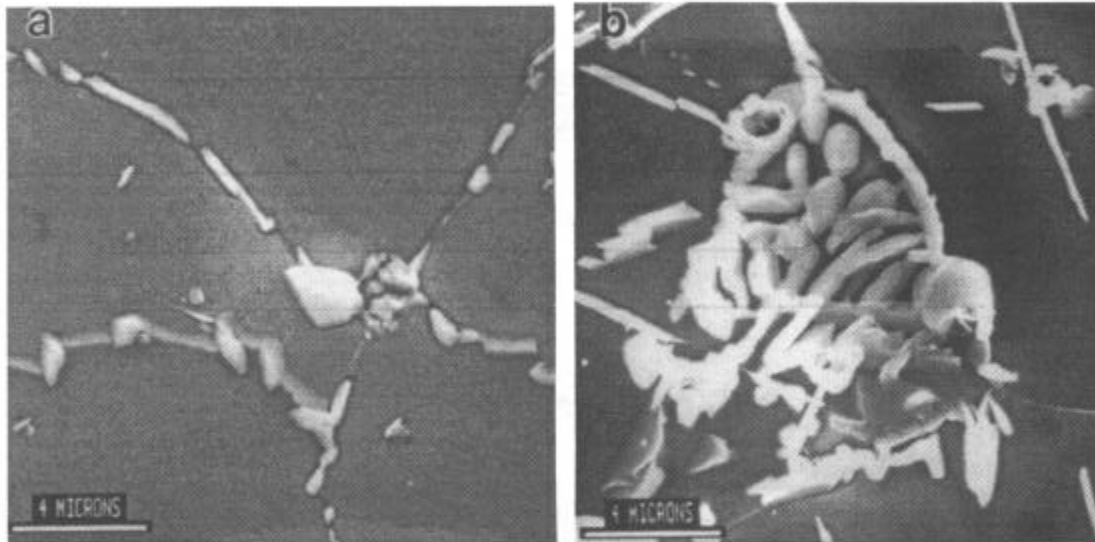


Figure 7 - SEM views of PIM alloy 718 sintered at a heating rate of 15°C/min showing Laves phase at the grain boundaries: (a) conventionally HT (b)  $\delta$ -phase heat treated.

#### Other Mechanical Properties.

High-cycle fatigue (HCF) and creep testing were conducted in the PIM HIP+HT materials at 650°C. The results were compared to the AMS 5696 minimum requirements.

The HCF results obtained at an R ratio of -1 indicated that the PIM material has a higher fatigue life than the AMS 5696 minimum requirements. A fatigue stress of 448.2 MPa at  $10^7$  cycles was determined in the PIM material. This is 37% above the AMS 5696 minimum requirements (326.8 MPa).

The creep properties for the PIM HIP+HT at 551.6 MPa with a total strain of 1% exceeded the AMS 5696 minimum specification (30 hours) by at least a factor of 2. However, the PIM specimens showed a wide range of time (30-to-123 hours) required to achieved a 1% strain. The wide range in time observed may be attributed to two main parameters which include (1) the non-uniform grain size of the PIM specimens (Table III), and (2) the non-uniform distribution of  $\delta$ -phase. Note that HCF and creep were not measured for the PIM materials heat-treated in the  $\delta$ -phase field.

#### Summary and Conclusions

The results of this work show that PIM alloy 718 can be successfully processed to meet the requirements stipulated for aerospace components in demanding applications. On the basis of the results obtained, the following conclusions can be made:

1. Sintering of PIM alloy 718 is complicated by the formation of eutectic-Laves phases which have a detrimental effect on the mechanical properties.
2. A small proportion of Laves phases and higher density in PIM material was obtained at a heating rate of 15°C/min.
3. The best combination of tensile properties at in the HIP+HT condition was obtained at a heating rate of 15°C/min.

4. The stress rupture ductility at 650°C increased as the  $\delta$ -phase content increased.
5. The tensile, stress rupture, creep, and high-cycle fatigue properties of the PIM material exceeded the AMS 5596 minimum requirements.

#### References

1. W. Track and W. Smarsly, "Injection Molding of High Temperature Materials," (Paper presented at the '93 Powder Injection Molding Symposium, Boulder, Co. Oct. 1993), 4-6.
2. J. J. Valencia, T. McCabe, K. Hens, J. O. Hansen, and A. Bose, "Microstructure and Mechanical Properties of Alloy 625 and 718 Process by PIM" (Paper presented at the Superalloys 718, 625, 706, and Various Derivatives Symposium, Warrendale, PA, 1994), Edited by E. Loria, TMS, p 935.
3. R. Scheemes, J. R. Spirko, and J. J. Valencia, "Powder Injection Molding of Inconel 718 Aerospace Components" (Advanced Particulate Materials And Processes Conference, West Palm Beach, FL (to be published)), MPIF.
4. The Engineering Society for Advancing Mobility Land Sea Air and Space International, Aerospace Material Specification (AMS 5662G, Jan. 1993).
5. A. Bose, private communication, Parmatech Corporation, Pataluma, CA, June 1994.
6. M. J. Cieslak, et. al., "The Solidification Metallurgy of Alloy 718 and Other Nb-Containing Superalloys" (presented at the Superalloy 718-Metallurgy and Applications Conference, Warrendale, PA, 1989), Edited by E. Loria, TMS, pp 59-68.
7. G. H. K. Bouse, "Application of a Modified Phase diagram to the Production of Cast Alloy 718 Components" (presented at the Superalloy 718-Metallurgy and Applications conference, Warrendale, PA, 1989), Edited by E. Loria, TMS, pp 69-77.
8. M. G. Burke and M. K. Miller, "Precipitation in Alloy 718: A Combined AEM and APFIM Investigation" (presented at the Superalloys 718, 625 and various Derivatives Symposium, Warrendale, PA, 1991), Edited by E. Loria, TMS, pp 337-350.
9. A. Oradei-Basile and J. F. Radavich, "A Current T-T-T Diagram for Alloy 718" (presented at the Superalloys 718, 625, 706, and various Derivatives Symposium, Warrendale, PA, 1991), Edited by E. Loria, TMS, pp 325-335.
10. J. H. Moll, G. N. Maniar, and D. R. Muzyka, "Heat Treatment of 706 Alloy for Optimum Stress - Rupture Properties," Metall. Trans., 2 (1971), 2153-2160.
11. Private communication, Pratt and Whitney, Palm Beach, FL, 1996.
12. Y. Desvallees, M. Bouzidi, F. Bois, and N. Beade, "Delta Phase in Inconel 718: Mechanical Properties and Process Requirements" (presented at the Superalloys 718, 625, 706, and various Derivatives Symposium, Warrendale, PA, 1994), Edited by E. Loria, TMS, pp 281-291.